

which are the most mature in terms of their evolutionary development, although it is widely recognized that column liquid chromatography still lacks a sensitive and universal detector for general applications. This void may be filled by mass spectrometry, which has made great strides in the last few years towards this goal based on particle-beam interfaces and atmospheric ionization techniques coupled with the development of low cost mass separators. By comparison, thin-layer chromatography and supercritical fluid chromatography have become recognized as techniques with niche applications and are unlikely to supplant gas and column liquid chromatography as the dominant chromatographic methods used in analytical laboratories. The microcolumn techniques of capillary electrophoresis, micellar electrokinetic chromatography, and capillary electrochromatography have quickly established themselves as useful laboratory methods and are likely to become of increasing importance as they complete their evolutionary cycle. In particular, the infant capillary electrochromatography has the potential to replace column liquid chromatography from many of its traditional separation roles, but has yet to reach a state of development to be considered as a routine laboratory technique.

The only thing that is certain about science is uncertainty. Although chromatographic methods are likely to dominate separation science for the first part of the twenty-first century, it would be a foolish person who predicts their form, continuing development, and main applications. Throughout the history of chromatography general approaches have had to adapt to changing needs brought about by dramatic shifts in the focus on different types of applications, and this has a significant impact on the relative importance of the various techniques. However, chromatography should be considered as an holistic

approach to separations, and will be better understood and correctly employed if we abandon the current trend to compartmentalize the technique based on specialization in individual subject areas.

See Colour Plate 3.

Further Reading

- Berger TA (1995) *Packed Column Supercritical Fluid Chromatography*. Cambridge: Royal Society of Chemistry.
- Braithwaite A and Smith FJ (1996) *Chromatographic Methods*. London: Blackie Academic & Professional.
- Giddings JC (1991) *Unified Separation Science*. New York: Wiley-Interscience.
- Guiochon G and Guilleman CL (1988) *Quantitative Gas Chromatography for Laboratory Analysis and On-Line Process Control*. Amsterdam: Elsevier.
- Guiochon G, Shirazi SG and Katti AM (1994) *Fundamentals of Preparative and Nonlinear Chromatography*. Boston: Academic Press.
- Heftmann E (1992) *Chromatography*, Parts A and B. Amsterdam: Elsevier.
- Jennings W, Mittlefehldt E and Stremple P (1997) *Analytical Gas Chromatography*. San Diego: Academic Press.
- Lee ML, Yang FJ and Bartle KD (1984) *Open Tubular Column Gas Chromatography. Theory and Practice*. New York: Wiley-Interscience.
- Li SFY (1992) *Capillary Electrophoresis. Principles, Practice and Applications*. Amsterdam: Elsevier.
- Poole CF and Poole SK (1991) *Chromatography Today*. Amsterdam: Elsevier.
- Robards K, Haddad PR and Jackson PE (1994) *Principles and Practice of Modern Chromatographic Methods*. London: Academic Press.
- Sherma J and Fried B (1997) *Handbook of Thin-Layer Chromatography*. New York: Marcell Dekker.
- Snyder LR, Kirkland JJ and Glajch JL (1997) *Practical HPLC Method Development*. New York: J Wiley.

CRYSTALLIZATION



H. J. M. Kramer and G. M. van Rosmalen,
Delft University of Technology, Delft, The Netherlands

Copyright © 2000 Academic Press

Introduction

Crystallization from solution is a separation technique where a solid phase is separated from a mother liquor. In contrast to other separation processes,

however, the dispersed phase consisting of numerous solid particles also forms the final product, that has to meet the required product specifications. Crystallization can thus also be seen as a technique to obtain solid products, where the crystallization process has to be carefully controlled in order to meet the ever-increasing demands of the customer on particle properties like particle size distribution, crystal shape, degree of agglomeration, caking behaviour and purity. Since the particles must also be easily

separated from the mother liquor, additional demands on filterability and washability can be formulated.

Because of the mostly rigid structure of the solid phase, the formation of solid particles is a rather slow process, and to reach an acceptable production rate large vessels are generally needed. This rigid structure on the other hand impedes the incorporation of foreign substances or solvent molecules, and in only one separation step a pure solid product is obtained.

Crystallization is often used as a generic term for evaporative or cooling crystallization, precipitation and melt crystallization. There are, however, considerable differences between the three types of crystallization as far as the processing method and the corresponding equipment are concerned. In precipitation the drop-out of the solid phase is achieved by mixing two feed streams that are either two reactants or a solvent containing the solute and an antisolvent. The hydrodynamics of the process therefore play a predominant role in precipitation with regard to the properties of the obtained product.

In melt crystallization the potential of crystallization to produce a pure product is mainly utilized, and the solid phase is remolten to obtain the final product. The applications are mainly in the ultrapurification of organic compounds or to produce pure water as a concentration technique.

An upcoming technique in crystallization is supercritical crystallization, mostly with condensed CO₂, because of its benign properties compared to organic solvents. Condensed CO₂ can be used either as a solvent or as an antisolvent, and specifically adapted processes and equipment have been developed for these high pressure crystallization techniques.

Also the crystallization of proteins requires its own dedicated approach, because large, sometimes easily degradable molecules require carefully designed processes.

Because 70% of the products sold by the process industry and the pharmaceutical industry – as bulk products, intermediates, fine chemicals, biochemicals, food additives and pharmaceutical products – are solids, crystallization in its widest definition is the largest separation process after distillation.

Although this chapter will primarily focus on evaporative and cooling crystallization, the energy, mass and population balances treated here as well as the kinetic rate expressions for the physical processes such as nucleation, growth and agglomeration and the characterization of the particles can equally be applied to the other types of crystallization.

Several books on the diverse aspects of crystallization have been published over the last 10 years. These books that can be recommended for a wide overview

in this field contain an abundance of references. The authors of these books are Mersmann (1995), Mullin (1993), Randolph and Larsen (1987), Myerson (1993), Nývlt (1992), Tavare (1995) and Hurle (1993). Söhnel and Garside (1992) have written a book on precipitation and Arkenbout (1995) a book on melt crystallization.

This article reviews industrial evaporation and cooling crystallization processes. A basic modelling approach is presented which enables the analysis and design of industrial crystallization processes, either by analytical calculations or by making use of modern computational tools.

Crystallization Methods and Supersaturation

Crystallization only occurs when supersaturation is created that acts as the driving force for crystallization. The crystallization method is mainly chosen on the basis of the thermodynamic and physical properties of the compound and the solvent, as well as on the required purity of the product. There are several ways to represent the phase diagram, depending on the mode of crystallization. For evaporative and cooling crystallization a solubility diagram is mostly used, in which the solubility of the compound is expressed as a function of temperature. In precipitation the solubility is always very low, and the solubility product at the operating temperature is needed. In antisolvent precipitation, the solubility diagram mostly has to be determined for the particular three-phase system. In melt cooling crystallization T - x diagrams are used, while for melt pressure crystallization pT - x diagrams are needed.

A decision scheme for the selection of the appropriate crystallization method is presented in **Figure 1**. For a high purity product or when the use of a solvent poses environmental or safety problems, melt crystallization is chosen. A melt temperature lying between 0 and 100°C is preferred, since at higher temperatures many organic compounds become unstable, while at temperatures below 0°C operating the process becomes more difficult, although not impossible. A high viscosity of the melt hampers the operation.

At solubilities below about 1 mass %, the process is designed as a precipitation process to obtain a reasonable production rate. The supersaturation that is generated by the mixing of reactants often reaches high values. Also in antisolvent crystallization, low solubility of the solute and high supersaturation are reached by mixing two solvents.

Finally, for the more easily soluble substances the choice between cooling and evaporative crystallization

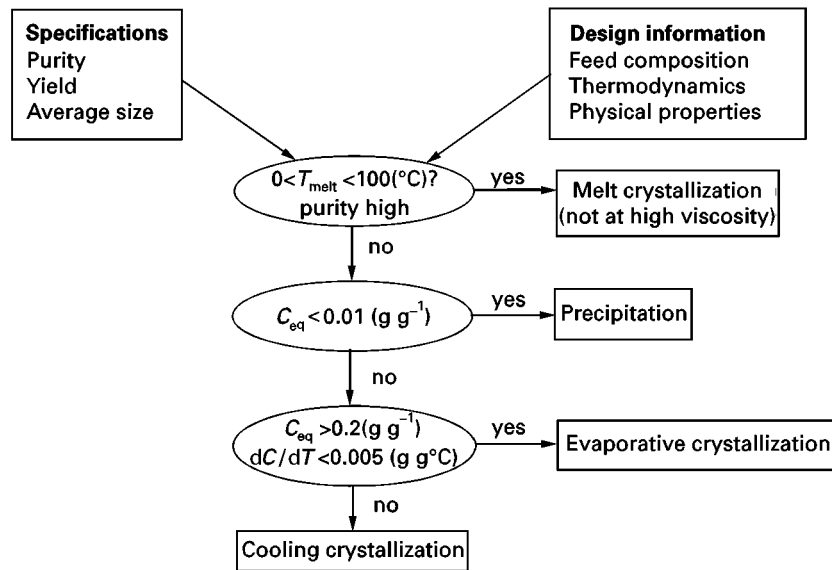


Figure 1 Decision diagram for choosing the method of crystallization.

is made on the basis of the solubility curve, and the prevailing supersaturations are generally low. Especially where water is the solvent, cooling crystallization is more favourable than evaporative crystallization, except for highly soluble substances. Therefore, multi-effect flash evaporation where the vapour is used for heating next crystallizer or the feed stream is frequently applied to reduce the energy costs, if evaporative crystallization is applied.

In cooling crystallization direct cooling, flash cooling or indirect cooling can be applied. Where indirect cooling is used encrustation on the cooling surfaces must be minimized. In flash cooling this problem is largely avoided at the expense of a more complicated installation. Also direct cooling uses an inert cooling medium or refrigerant that is bubbled directly into the solution and evaporates does not suffer from abundant incrustation, but needs recompression of the cooling medium.

So, in these various methods of crystallization, supersaturation is created by cooling, by evaporation of solvent or by a combination of the two in the case of flash evaporation or flash cooling, or by mixing two reactants or solvents. In all these cases the actual concentration is higher than the equilibrium concentration, and a driving force for crystallization is achieved.

From a thermodynamic point of view this driving force is reflected by the difference in chemical potential of the solute in the liquid and in the solid phase at temperature T :

$$\Delta\mu = \mu_L(T) - \mu_S(T) \quad [1]$$

For cooling crystallization from the melt or the solution, eqn [1] can be transformed into:

$$\Delta\mu = \frac{\Delta H_{\text{eq}}}{T^*} \cdot \Delta T \quad [2]$$

For melt pressure crystallization:

$$\Delta\mu = \Delta V_{\text{molar}} \Delta P = \frac{\Delta\rho}{\rho_{\text{melt}}\rho_{\text{solid}}} \cdot \Delta P \quad [3]$$

For practical reasons the supersaturation in cooling is mostly indicated by:

$$\Delta T = T - T^* \quad [4]$$

and can also be translated via the solubility curve into a concentration difference:

$$\Delta c = c - c^* \quad [5]$$

Other frequently used expressions are the dimensionless saturation ratio:

$$S = \frac{c}{c^*} \quad [6]$$

or the relative supersaturation:

$$\sigma = \frac{c - c^*}{c^*} = \frac{\Delta c}{c^*} = S - 1 \quad [7]$$

Here c can be expressed by kg solute per kg or m^3 of the solvent or solution, but an expression in kg solute per m^3 solution (=liquid) phase is generally used in mass balances (=mass fraction, w).

For evaporative crystallization, eqn [1] can be transformed into:

$$\Delta\mu = RT \ln\left(\frac{a}{a_{\text{eq}}}\right) = RT \ln\left(\frac{\gamma c}{\gamma_{\text{eq}} c^*}\right) \quad [8]$$

Given the relatively low supersaturations, σ , that often lie between 0.001 and 0.01 with more easily soluble substances, eqn [8] simplifies into:

$$\Delta\mu = RT \frac{\Delta c}{c^*} = RT\sigma \quad [9]$$

For two or more A and B ions in solution that react to form crystal c , the expression for $\Delta\mu$ becomes:

$$\Delta\mu = RT \ln \frac{\prod_i a_i^{\nu_i}}{K_{\text{sp}}} \quad [10]$$

and for stoichiometric solutions equals:

$$\Delta\mu = RT\nu \ln S \approx RT\nu\sigma \quad [11]$$

In practice the supersaturation is often indicated by eqn [5].

For flash cooling or evaporation two terms contribute to the driving force (ΔT and Δc).

For precipitation, no simplifications are allowed, owing to the high supersaturation values ($\sigma \gg 1$), and either eqn [8] or eqn [10] is used. For antisolvent precipitation the value of c depends on the actual concentration of the solute in the original solvent and, like c^* , on the degree of dilution by the antisolvent.

Mass and Heat Balances

Traditional design of an industrial crystallizer is based on only mass and enthalpy balances. The production rate determines to a large extent the dimensions of the crystallizer as well as the energy consumption. It also determines the mode of operation, which means batchwise or continuous, single or multistage operation. In the next section the balance equations are given for an evaporative and for a cooling crystallizer.

Evaporative Crystallizers

Consider an ideally mixed vessel. The composition of the product stream is kept similar to that of the

content of the crystallizer. The volume, V , of the crystallizer is often assumed to be constant in eqns [12–19]. However, by making V and the feed streams time-dependent, dynamic effects can be taken into account, and thus also batch processes. The mass balance is given by:

$$\begin{aligned} \frac{dM_{\text{total}}}{dt} = & \phi_{v,\text{feed}}(\varepsilon_{\text{feed}}\rho_{\text{feed,liquid}} + (1 - \varepsilon_{\text{feed}})\rho_{\text{crystal}}) \\ & - \phi_{v,\text{prod}}(\varepsilon\rho_{\text{liquid}} + (1 - \varepsilon)\rho_{\text{cryst}}) - \phi_{v,\text{vapour}}\rho_{\text{vapour}} \end{aligned} \quad [12]$$

The component balances are given by:

$$\begin{aligned} \frac{dM_i}{dt} = & \phi_{v,\text{feed}} \left(\varepsilon_{\text{feed}}\rho_{\text{feed,liquid}}w_{\text{feed,liquid},i} \right. \\ & \left. + (1 - \varepsilon_{\text{feed}})\rho_{\text{crystal}}w_{\text{feed,crystal},i} \right) \\ & - \phi_{v,\text{prod}}(\varepsilon\rho_{\text{liquid}}w_{\text{liquid},i} + (1 - \varepsilon)\rho_{\text{crystal}}w_{\text{crystal},i}) \end{aligned} \quad [13]$$

($i = 1, N_{\text{comp}}$)

with:

$$M_i = V(\varepsilon\rho_{\text{liquid}}w_{\text{liquid},i} + (1 - \varepsilon)\rho_{\text{crystal}}w_{\text{crystal},i}) \quad [14]$$

where component $i = 1$ is the main compound to be crystallized, and components $i = 2, 3, \dots, N_{\text{comp}}$ are the impurities present.

The distribution coefficients relate the impurity uptake by the solid and the concentration of the impurity in the liquid phase:

$$k_{\text{distr},i} = \frac{w_{\text{crystal},i}}{w_{\text{liquid},i}} \quad (i = 2, \dots, N_{\text{comp}}) \quad [15]$$

Instead of substituting all component balances into the total mass balance given by eqn [12] to solve the mass balance of the total system, it is more convenient to combine the solvent mass balance together with the component balances:

$$\begin{aligned} \frac{dV\varepsilon\rho_{\text{liquid}}w_{\text{liquid,solvent}}}{dt} = & \phi_{v,\text{feed}}(\varepsilon_{\text{feed}}\rho_{\text{feed,liquid}}w_{\text{feed,solvent}}) \\ & - \phi_{v,\text{prod}}(\varepsilon\rho_{\text{liquid}}w_{\text{liquid,solvent}}) \\ & - \phi_{v,\text{vapour}}\rho_{\text{vapour}} \end{aligned} \quad [16]$$

Finally, the sum of the mass fractions in both the liquid and the solid phase must equal one:

$$w_{\text{liquid,solvent}} + \sum_i w_{\text{liquid},i} = 1 \quad [17]$$

$$\sum_i w_{\text{crystal},i} = 1 \quad [18]$$

The enthalpy balance with the production rate or solids production, P , is given by:

$$\frac{dH}{dt} = \phi_{H,feed} - \phi_{H,prod} - \phi_{H,vapour} + Q_{heat} + P\Delta H_{cr} \quad [19]$$

The total enthalpy and the enthalpy of the streams are defined as:

$$\begin{aligned} H &= V(\varepsilon\rho_{liquid}C_{p,liquid} + (1 - \varepsilon)\rho_{crystal}C_{p,crystal})T \\ \phi_{H,feed} &= \phi_{v,feed}(\varepsilon_{feed}\rho_{feed,liquid}C_{p,liquid} \\ &\quad + (1 - \varepsilon_{feed})\rho_{crystal}C_{p,crystal})T_{feed} \\ \phi_{H,prod} &= \phi_{v,prod}(\varepsilon\rho_{liquid}C_{p,liquid} + (1 - \varepsilon)\rho_{crystal}C_{p,crystal})T \\ \phi_{H,vapour} &= \phi_{v,vapour}(\rho_{vapour}C_{p,vapour}T + \rho_{vapour}\Delta H_{evap}) \end{aligned} \quad [20]$$

The crystal free volume fraction ε should be as low as possible to reduce the crystallizer volume.

The liquid mass fraction $w_{liquid,1}$ of the main component must be determined or can be approximated by the saturation concentration, especially for soluble compounds with a low σ value.

With the production rate, P , as a design parameter, the volumetric product flow rate can be deduced for the chosen ε value from:

$$P = \phi_{v,prod}(1 - \varepsilon)\rho_{crystal} = \phi_{v,prod}M_T \quad [21]$$

From the product flow rate so obtained and the mean residence time that is needed to grow sufficiently large crystals, the necessary suspension volume for the crystallizer can be calculated from:

$$\phi_{v,prod} = \frac{V}{\tau} \quad [22]$$

$$\tau = \frac{L_{mean}}{4G_{mean}} \quad [23]$$

Here, for the desired L_{mean} , a reasonable value must be chosen, that is related to its solubility and the mean growth rate, G_{mean} , can be estimated from a correlation (Mersmann, 1988; Kind and Mersmann 1990) or determined by laboratory experiments.

From the crystallizer suspension volume, V , the needed vapour head, the process streams and the heat duty that has to be accommodated, the crystallizer dimensions can now be determined. Constraints for the design are a height/diameter ratio of about 3 : 2, and a cross-sectional area for evaporation that is large enough to avoid entrainment of liquid droplets

into the condenser. For the design of the heat exchanger see Sinnott (1998).

Cooling Crystallizers

In cooling crystallization the warm feed stream is cooled to the process temperature. In principle the same set of mass and heat balance equations can be used, except that no vapour flow exists. Furthermore, the process temperature cannot freely be chosen, because it is determined for a given production rate, crystal free fraction, ε , residence time, τ and liquid mass fraction, $w_{liquid,1}$. This latter liquid mass fraction of the main component will depend on the process temperature, so a temperature-dependent equation for $w_{liquid,1}$ must be added. The degrees of freedom for the crystallizer design are therefore more limited.

The Population Balance

The Crystal Length-based Population Balance Equation

In crystallization as a separation process, the separability of the particles from the mother liquor by, for example, filtration are of utmost importance, as well as their washability and drying. The efficiency of these processes is directly related to the crystal size distribution (CSD) of the solid, and as soon as the CSD of the solid phase becomes an interesting product specification, the population balance equation (PBE) must be introduced. The PBE describes how the size distribution develops in time as a result of various kinetic processes. The concept of the PBE was introduced to crystallization by Randolph. A general form of the PBE is as follows:

$$\begin{aligned} \frac{\partial(n(L)V)}{\partial t} &= -V\frac{\partial(G_L(L)n(L))}{\partial L} + B(L)V - D(L)V \\ &\quad + \sum_{j=1}^m \phi_{v,in,j}n_{in,j}(L) - \sum_{k=1}^n \phi_{v,out,k}b_{out,k}(L)n(L) \end{aligned} \quad [24]$$

where the amount and the size of the crystals (or particles) are expressed in terms of number density $n(L)$ ($\#/(m^3m)$) and crystal (or particle) length L (m) respectively (Figure 2A).

All the variables in this equation are in principle also time-dependent. For the sake of simplicity, the t dependence is omitted here.

In other representations of the PBE, the amount of particles may also be expressed in terms of volume density $\nu(L)$ ($m^3/(m^3m^1)$) or mass density $m(L)$ ($kg/(m^3m^1)$, where the size is represented by the

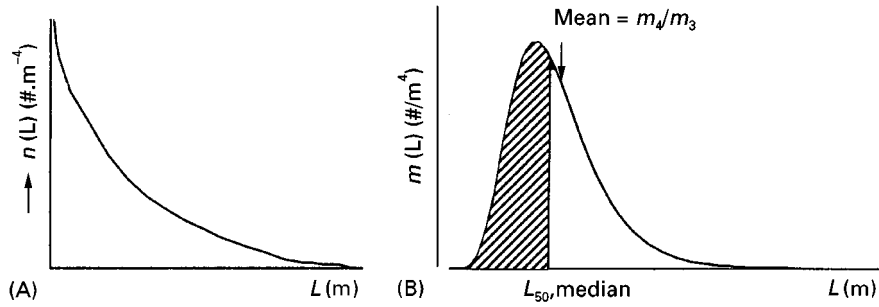


Figure 2 (A) Number and (B) mass distribution of a crystal population.

length L (Figure 2B). Figure 2 also shows two often-used values which characterize the crystal size distribution, the mean crystal size and the volume-based median size (the size at which the integral over the $m(L)$ curve from zero to L_{50} equals half of the integral over the entire curve).

For particle sizes given in terms of volume, the corresponding number density becomes $n(v)$ instead of $n(L)$. The latter representation becomes more convenient if agglomeration of crystals plays an important role.

In eqn [24] V is the suspension volume in the crystallizer with m streams entering and n streams leaving the crystallizer with volumetric flow rates ϕ_v .

$G_L(L)$ is the linear size-dependent growth rate ($m\ s^{-1}$), and $B(L)$ and $D(L)$ are birth and death terms

respectively ($\#m^{-3}m^{-1}$). Birth and death events can be caused by agglomeration and disruption of earlier agglomerated particles, but also by breakage of crystals and by the birth of small crystals, called nuclei. Breakage of crystals will not happen under normal operating conditions.

The classification function $h(L)$ describes the relation between the CSD in the crystallizer and that on an outlet stream.

The processes on the right-hand side of eqn [24] that lead to the crystal population in a certain size interval, dL , are depicted in Figure 3. In the PBE given by eqn [24] all operation modes are represented. The difference between batch and continuous processes only influences the in- and outflow terms on the right-hand side of the PBE.

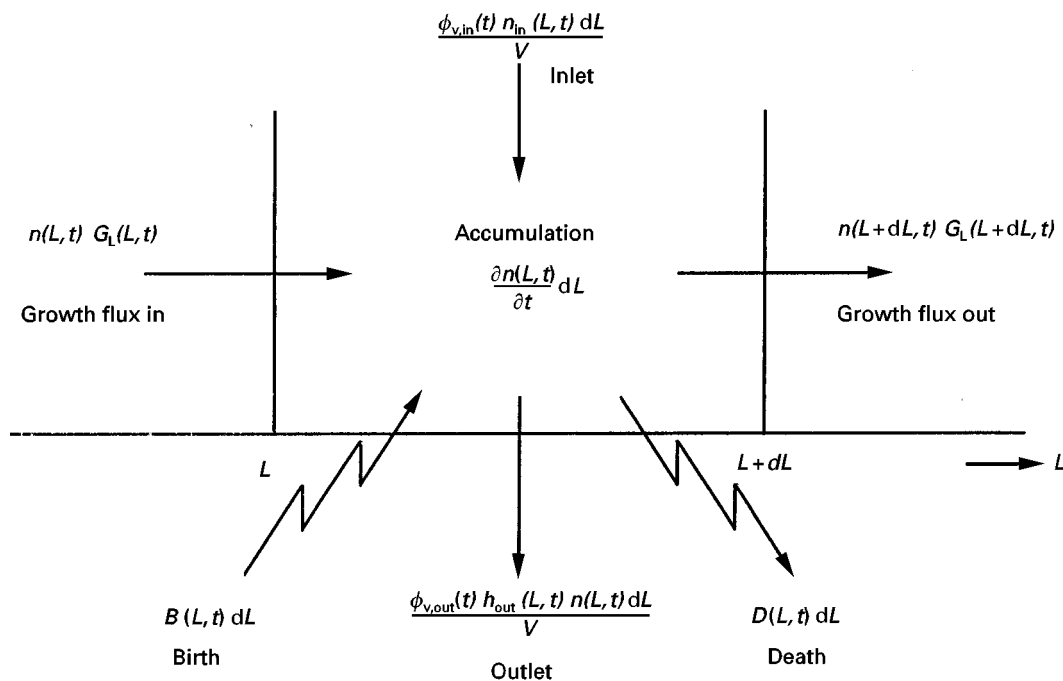


Figure 3 Schematic depiction of the processes affecting the CSD. In an infinitesimally small size range from L to $L + dL$, crystals may enter and leave due to growth, aggregation, attrition, breakage and volumetric input and output flow streams.

As the PBE is a partial differential equation with respect to time t and crystal length L , two boundary conditions are needed to solve it analytically:

$$n(0, t) = \frac{B_0}{G_L(0)} \quad [25]$$

$$n(L, 0) = \text{initial distribution} \quad [26]$$

As primary and secondary nucleation typically involve the birth of small crystals, nucleation is often presented as the birth of nuclei at zero size. Instead of a birth term in the PBE for the nucleation event $B(L)$ that happens over a size range $0 \leq L \leq y$, the birth rate B_0 given by the boundary eqn [25] is used. These two are related by:

$$B_0 = \int_0^y B(L) dL \quad [27]$$

For the second boundary condition, a seed population or a population formed by the outgrowth of primary nuclei can be substituted.

Population Balance Equation for Stationary Operation

For continuous crystallization the PBE can be simplified by assuming that:

1. a steady state is reached
2. there is one crystal-free inlet stream
3. nucleation only occurs at zero size and is given by the boundary condition at $L = 0$ (eqn [25])
4. growth is size-independent, $G_L(L) = G_L$
5. the crystallizer volume is constant in t
6. there is no agglomeration or breakage

This results in:

$$VG_L \frac{\partial n(L)}{\partial L} + \sum_{k=1}^n \phi_{v,\text{out},k} h_{\text{out},k}(L) n(L) = 0 \quad [28]$$

If the crystallizer content is also well mixed, and there is only one nonclassified outflow, i.e. $h(L) = 1$, this equation becomes:

$$VG_L \frac{\partial n(L)}{\partial L} + \phi_{v,\text{out}} n(L) = 0 \quad [29]$$

Such a crystallizer is named a mixed suspension mixed product removal (MSMPR) crystallizer.

Integration of eqn [29] leads to:

$$n(L) = n(0) \exp\left(-\frac{L}{G_L \tau}\right) \quad [30]$$

By plotting $\ln(n(L))$ versus L , the kinetic growth rate G_L can be derived from the slope of the straight line, and the nucleation rate B_0 from the intercept with the y axis.

The number of process parameters that can be varied for a specific crystallizer in order to shift the CSD and in particular the mean crystal size is usually very limited. Typical process actuators are fines removal and product classification. Their influence on the CSD can be analytically solved by introducing more classified outflow streams, which cause different residence times for the mother liquor and the fine, medium and large crystals in the crystallizer. A generic numeric solution is achieved more easily, as will be addressed later.

Moment Equations for Stationary and In-Stationary Operation

Analytical solutions of the PBE for in-stationary crystallizers hardly exist. By transforming the PBE into a moment form, however, analytical solutions are attained that allow us to describe the dynamical behaviour of crystallizers in terms of the moments of the distribution. The moments are defined as:

$$m_i = \int_0^\infty n(x) x^i dx \quad [31]$$

and the first five moments are related to measurable physical properties of the distribution, as shown in **Table 1**. The shape factors k_a and k_v relate the crystal length to its surface area and volume respectively.

For a continuously operated system with a constant V , a size-independent growth rate, no agglomeration, nucleation at zero size, one crystal-free inlet stream, and a nonclassified product stream, the PBE presented in eqn [24] transforms into:

$$\frac{\partial n(L)}{\partial t} = -G_L \frac{\partial n(L)}{\partial L} - \frac{n(L)}{\tau} \quad [32]$$

Table 1 Physical properties of the moments of the distribution

Property	Symbol	Moment equation
Total number	N_T	m_0
Total length	L_T	m_1
Total surface area	A_T	$k_a m_2$
Total volume	V_T	$k_v m_3$
Total mass	M_T	$\rho k_v m_3$

with similar boundary conditions. This equation can be reduced to a set of ordinary differential equations by means of the moment transformation:

$$\frac{dm_j}{dt} = jG_L m_{j-1} - \frac{m_j}{\tau} + B_0 L_0^j \quad [33]$$

where L_0 , the size of the nuclei, is here zero. Only the first four moment equations ($j = 0-3$) have to be solved to obtain all the information about the lumped properties of the CSD.

Population Balance Equation for Batch Operation

For batch operation, the PBE (eqn [24]) can be simplified by assuming that:

1. the inlet stream is crystal-free
2. nucleation only occurs at zero size, and is reflected by the boundary condition at $L = 0$ (eqn [25])
3. growth is size-independent
4. there is no agglomeration or disruption

This results in:

$$\frac{\partial n(L)V}{\partial t} = -VG_L \frac{\partial n(L)}{\partial L} \quad [34]$$

Since batch operation is inherently 'in-stationary', a moment transformation is needed to obtain analytical solutions to the PBE. This leads to

$$d \frac{d(Vm_j)}{dt} = jG_L m_{j-1} V + B_0 L_0^j V \quad [35]$$

where the size of the nuclei, L_0 , is zero. Again ordinary differential equations ($j = 0-3$) have to be solved to attain the lumped properties of the CSD.

To improve the CSD, a controlled cooling or evaporation trajectory can be imposed.

The Crystal Volume-Based Population Balance Equation

When a crystallizing system depends purely on nucleation and growth processes, it is favourable to use a PBE with length as the crystal size co-ordinate. For kinetic processes where the volume of particles are combined or split up, like in agglomeration and disruption, a PBE with the particle volume as crystal size coordinate is preferred. This leads to:

$$\begin{aligned} \frac{\partial(n(v)V)}{\partial t} = & -V \frac{\partial(G_v(v)n(v))}{\partial v} + B(v)V - D(v)V \\ & + \sum_{j=1}^m \phi_{v,in,j} n_{in,j}(v) - \sum_{k=1}^n \phi_{v,out,k} b_{out,k}(v)n(v) \end{aligned} \quad [36]$$

A volumetric growth rate is then required. Crystal growth rates are, however, available in length-based rates, so $G(v)$ has to be calculated from:

$$G_v(v) = \frac{dv}{dL} G_L = 3k_v L^2 G_L \quad [37]$$

This expression prohibits the introduction of zero-sized nuclei as a boundary condition, and nucleation has to be modelled as birth within a certain size interval.

The number of particles in a certain size interval must be the same, regardless of whether the bounds of that interval are expressed in terms of length of volume. This implies that:

$$n(L) dL = n(v) dv \quad [38]$$

and, after some rewriting, the following transformation equations:

$$n(L) = 3k_v L^2 n(v)$$

$$n(v) = \frac{1}{3\sqrt[3]{k_v v^2}} n(L) \quad [39]$$

Agglomeration and Disruption

To solve the PBE where there is agglomeration and disruption of earlier agglomerated particles, the birth and death terms for these processes must be derived.

The rate of agglomeration, r , is given by:

$$r(v_1, v_2) = \beta(v_1, v_2, \sigma, \varepsilon) n(v_1) n(v_2) \quad [40]$$

The rate constant, β , commonly called the agglomeration kernel, depends on the particle sizes v_1 and v_2 , the supersaturation σ and the turbulence level, represented by the power input ε . The birth and death terms associated with the agglomeration of two particles, resulting in the birth of a new one and the death of the original two, are:

$$B(v) = \frac{1}{2} \int_0^v \beta(u, v-u) n(u) n(v-u) du \quad [41]$$

$$D(v) = n(v) \int_0^\infty \beta(u, v) n(u) du \quad [42]$$

The factor $\frac{1}{2}$ is needed to avoid double-counting, since the integral takes each interaction twice. The dependency of β on σ and ε has been omitted here for notation simplicity.

There is also disruption of earlier agglomerated particles with a corresponding disruption rate. This disruption process of earlier agglomerated particles

can be described in the PBE by an additional death term for the disrupted particles, and an additional birth term for the newly formed particles:

$$D(v) = S(v, \varepsilon) \cdot n(v) \quad [43]$$

$$B(v) = \int_v^{\infty} b(v, u) S(u, \varepsilon) n(u) du \quad [44]$$

where $S(v)$ is a selection function that describes the rate at which particles fall apart, and b is a breakage function that describes how many particles of size v are formed on disruption of a particle of size u .

Often, the disruption terms are loaded into the agglomeration kernel β , which then represents the effective agglomeration kernel. In that case terms expressed by the eqns [43] and [44] can be left out and only eqns [41] and [42] are needed for substitution in the PBE. The main disadvantage of this lumped description of the whole agglomeration process is that prediction of the agglomeration behaviour for different hydrodynamic conditions (and thus for different scales and geometries) becomes virtually impossible because β and σ have a different dependency on ε .

The PBE with agglomeration and disruption terms can rarely be solved analytically. A moment transformation is again required with the moments defined as:

$$m_i = \int_0^{\infty} n(v) v^i dv \quad [45]$$

where v represents crystal size volume v . The zero moment is again the total number of particles, but the first moment of the volume-based CSD already equals the third moment of the length-based CSD.

Substitution of the above expressions into the PBE (eqn [36]) for a system with agglomeration and growth and no nucleation, with a constant crystallizer volume, only one crystal-free inlet stream and a nonclassified product stream, results after a moment transformation in:

$$\frac{dm_i}{dt} = -\frac{m_i}{\tau} + jG_v m_{i-1} + \overline{B_{\text{agg},j}} - \overline{D_{\text{agg},j}} \quad [46]$$

where the moment forms of B and D due to agglomeration are defined as:

$$\overline{B_{\text{agg},j}} = \int_0^{\infty} v^j B dv \quad [47]$$

$$\overline{D_{\text{agg},j}} = \int_0^{\infty} v^j D dv \quad [48]$$

A solution is only obtained for a size-independent kernel β_0 . For a batch-agglomerating system (without growth), only solutions for m_0 and m_1 (which is equal to the m_3 in size coordinates) are obtained:

$$\frac{dm_0}{dt} = -\frac{1}{2}\beta_0 m_0^2 \quad [49]$$

$$\frac{dm_1}{dt} = 0 \quad [50]$$

The numerical solution of the population balance for cases where nucleation, growth and agglomeration is present often imposes a problem, because no analytical solution exists and the generation of numerical solutions is not easy. It is essential to divide the size axis into proper size intervals to obtain reliable results and to transform the population balance, a partial differential equation, into a set of ordinary differential equations. Hounslow *et al.* presented a numerical scheme based on a geometrical discretization of the size axis in which for each size interval the ratio between the upper and lower boundary r is exactly equal to $\sqrt[3]{2}$. Although accurate results are obtained in the absence of crystal growth and nucleation, the method is in general not accurate enough in the presence of these crystallization phenomena and gives rise to an overestimation of the higher moments. An improved finite-element technique has been introduced to solve the steady-state solution of the population balance for nucleation, growth and agglomeration.

Kinetic Expressions

In order to solve the population balance equation, kinetic expressions are needed to represent the physical processes that take place in the crystallizer, such as nucleation, growth and agglomeration. Their mechanisms and the corresponding equations will be treated here.

Nucleation

Two different nucleation mechanisms can be distinguished: primary and secondary nucleation.

Primary nucleation is new phase formation from a clear liquid or solution. It can be subdivided into homogeneous and heterogeneous nucleation. In the latter case a foreign substrate of tiny invisible particles, e.g. dust or dirt particles, is present in the solution on which nucleation starts. In homogeneous nucleation such a substrate is absent and nuclei are formed by statistical fluctuations of solute entities that cluster together.

Secondary nucleation is the breeding of nuclei from crystals of the crystallizing material that are already present in the solution. These nuclei are in general attrition fragments, and result from collisions of the larger crystals with the hardware of the crystallizer, in particular with the blades of impellers and pumps. At high solid densities in the crystallizer collisions between the larger crystals can create fragments that act as secondary nuclei.

During the start-up phase of evaporative or cooling crystallization of moderately to very soluble compounds, primary nucleation takes place. After their outgrowth to larger crystals, secondary nucleation takes over, and becomes the most important source of nuclei at low supersaturation values. For precipitation of slightly soluble compounds the process generally remains dominated by primary nucleation for two reasons. Supersaturation remains high enough, especially at the inlet points of the feed streams, to produce primary nuclei, and the often agglomerated crystals remain too small to be prone to attrition.

Homogeneous primary nucleation Local fluctuations in concentration induce the formation of numerous clusters that can fall apart again. In under- or just saturated solutions, cluster formation and cluster decay are in equilibrium; it is a reversible process. In supersaturated solutions, however, clusters of a critical size are formed that either fall apart or grow out. In the classical nucleation theory of Volmer, Becker and Döring, these clusters are formed by the attachment and detachment of single solute entities. Although clusters can also grow by the collision of clusters, their concentration is always so much lower than that of single solute entities that this process of cluster enlargement can be ignored.

The critical size of a cluster that is represented by its critical radius, r^* , is given by:

$$r^* = 2\gamma \frac{V_{\text{molar}}}{\Delta\mu} \quad [51]$$

and is thus related to the supersaturation via $\Delta\mu$, and to the interfacial tension γ .

For the homogeneous nucleation rate, J_{homo} ($\#m^{-3}$), the following equation can be derived after some simplifications:

$$J_{\text{homo}} = AS \exp\left(\frac{16\pi\gamma^3 V_{\text{molar}}^2}{3k^3 T^3 (\ln S)^2}\right) \quad [52]$$

In this Arrhenius type of expression, changes in the supersaturation ratio S in the pre-exponential factors $A \cdot S$ are of minor influence compared to changes in S in the exponential term. Various authors use dif-

ferent expressions for A and this can cause considerable differences in the attained values of J (Merzmann, 1995; Söhnel and Garside, 1992; Kashchiev, 2000).

Heterogeneous primary nucleation The occurrence of homogeneous nucleation is rare, in practice since nucleation on a foreign substrate will substantially reduce the nucleation barrier. For this type of nucleation, a similar rate equation can be used:

$$J_{\text{hetero}} = A_{\text{hetero}} S \exp\left(\frac{16\pi\gamma^3 V_{\text{molar}}^2}{3k^3 T^3 (\ln S)^2}\right) \quad [53]$$

where the interfacial tension γ is replaced by a much lower γ_{eff} . Although A_{hetero} is lower than A , the effect of the exponential term dominates up to very high supersaturation values, that are rarely met in practice (Figure 4).

Secondary nucleation The classic expression for the secondary nucleation rate in a suspension of growing crystals, B_0 , is the empirical power law, based on three experimentally accessible parameters that were recognized already early on to be important:

$$B_0 = k_N G^i N^h M_T^j \quad [54]$$

Since the growth rate is directly related to the supersaturation σ , and the rotational speed to the power input, the power law can also be written as:

$$B_0 = k_N^1 \sigma^b \varepsilon^k M_T^j \quad [55]$$

Frequently measured values for b , k and j under steady-state conditions are $1 < b < 3$, $0.6 < k < 0.7$ and $j = 1$ or 2 . For nucleation dominated by crystal-impeller collisions $j = 2$, while for nucleation ruled by crystal-crystal collisions, $j = 2$.

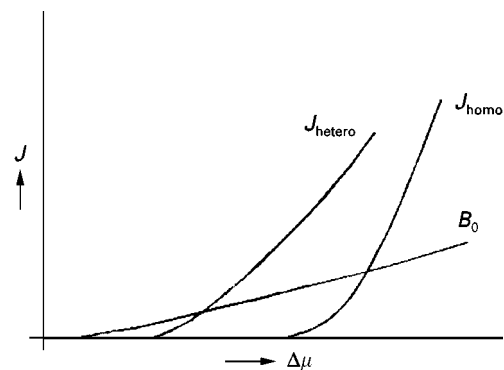


Figure 4 Nucleation rate as a function of the supersaturation ($\Delta\mu$). J_{homo} and J_{hetero} , homogeneous and heterogeneous nucleation rate; B_0 , secondary nucleation rate.

Also the crystallizer geometry-like type of stirrers or pumps, and number of blades, as well as the scale of operation influence the attrition rate of the crystals. These effects were supposed to be included in k_N of k_N^1 , that could only be established experimentally. The power law with its four parameters, used together with other kinetic parameters (e.g. those related to the growth of the crystals) seems to be perfectly adequate to describe the steady-state median crystal size in continuous crystallization processes.

The power law, however, fails to describe the dynamics of a crystallization process. If, for example, the median crystal size is plotted versus time from immediately after the start-up, often an oscillating behaviour is observed that dampens out until finally a steady-state value is reached (Figure 5). This oscillating behaviour can be explained by the observation that only crystals above a certain size breed secondary nuclei by attrition. The first nuclei are created by primary nucleation and grow out, which causes the supersaturation to decrease. When the mean size has reached its first peak, more of the larger crystals are withdrawn with the product than are grown into the larger crystal sizes by outgrowth of secondary nuclei. This happens because at the early stages no large crystals are available for breeding.

Some groups have tried to account for this phenomenon by adding a target efficiency to the power law that is a function of the crystal size. One author, Eek, allowed only crystals above a certain size to breed. This improved the simulations, although none of them was fully successful.

An attrition function for the crystals, was introduced by O'Meadhra based on the approach of Mersmann. He distributed the attrited volume over the small crystal sizes. In this way a birth function $B(L)$ was calculated from the volumetric attrition rate. A disadvantage of this modelling, in common with the power law, is that it has no predictive value, since

the attrition function also must be determined experimentally for the particular crystallizer.

Gahn and Mersmann were the first to derive a secondary nucleation rate model based on physical attrition properties. Their approach comprises three consecutive steps and calculates the secondary nucleation rate of crystals that collide with the blades of an impeller.

1. A simplified flow pattern based on geometric considerations as presented by Ploss *et al.* is used to calculate the impact velocity and the chance of crystals from size class i to collide with an impeller segment j .
2. Subsequently a model was developed to calculate the volume of attrition fragments produced during a single collision of a crystal corner represented by a cone, and a hard flat surface of the impeller. The model relates the attrited volume of crystal i and segment j to the impact energy of the crystal collision via its relevant mechanical properties, such as the Vickers hardness, the fracture resistance of the substance and the shear modulus. The model assumes that the circulation time is sufficient to heal the damaged crystal corner before a subsequent collision of the same corner takes place. This assumption is often not valid for crystallizers up to 100 L. A minimum impact energy required to cause fracture can also be derived, and thus the minimum crystal size for a given velocity profile is prone to attrition. The model also provides a normalized number density function of the fragments formed at each collision of crystal i with impeller segment j . In general, the size distribution of fragments lies in the range from 2 to 100 μm .
3. In the third step the rate of secondary nucleation is linked to the rate of formation of attrition fragments. The amount of stress remaining in the fragments limits the number that grows into the population, because stress increases their chemical potential. Their real saturation concentration c^* becomes:

$$c_{\text{real}}^* = c^* \exp\left(\frac{\Gamma_K}{KTL_{\text{fragment}}}\right) \quad [56]$$

The stress content of the fragments is directly related to their length, and the value of Γ_K has to be determined experimentally, for example from experiments where the fines of a crystallizer are withdrawn, and allowed to grow out in a growth cell.

The formed fragments with size L_{fragment} can now be distributed with their respective length and stress content. A number of fragments will dissolve, and the

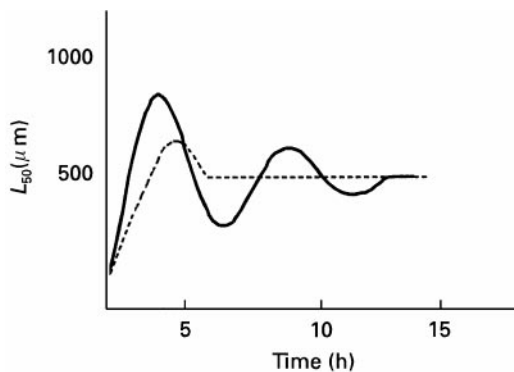


Figure 5 Dynamic behaviour of the CSD. Continuous line, measured; dashed line, modelled with the power law.

rest will grow into the population with a size-dependent growth rate.

This model does not deliver a secondary nucleation rate, B_{0s} , with nuclei born at zero size or a birth term, $B(L)$, for the distribution of secondary nuclei, but calculates from the number of collisions, and from the surviving fragments per collision, the number of new developing crystals. Since for this calculation an initial CSD is needed, iteration loops are always needed if this nucleation model is used as a predictive tool for secondary nucleation.

Both this model and that of O'Meadhra are able to describe the dynamic behaviour of crystallization processes.

Crystal Growth

Definitions of growth rate The growth rates of the crystallographically different faces ($h k l$) of a crystal can vary considerably. The growth rates of the crystal faces determine the shape of the crystal and, together with the growth mechanisms, also the crystal surface structure.

The growth rate of a particular crystal face ($h k l$) is mostly defined by its linear growth rate R_{lin} ($m s^{-1}$), which refers to the growth rate of that face along the normal direction. An overall linear growth rate \bar{R}_{lin} averaged over all different ($h k l$) faces can be defined in several ways. One definition which is often used relates \bar{R}_{lin} to the increase of the crystal mass in time:

$$\frac{1}{A} \frac{dm}{dt} = \frac{\rho k_v}{k_a L^2} \frac{dL^3}{dt} = 3 \frac{k_v}{k_a} \rho G_L = 6 \frac{k_v}{k_a} \rho \bar{R}_{lin} \quad [57]$$

For spheres and cubes (or for crystals where L is based on the diameter of a sphere with the same volume), $k_a/k_v = 6$, and:

$$\frac{1}{A} \frac{dm}{dt} = \frac{1}{2} \rho G_L = \rho \bar{R}_{lin} \quad [58]$$

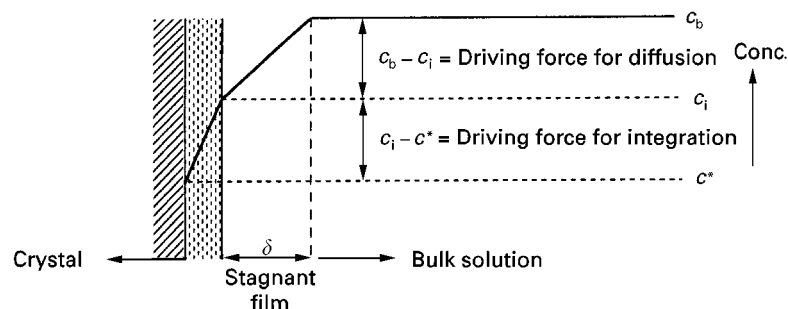


Figure 7 Concentration profile perpendicular to the crystal surface during growth.

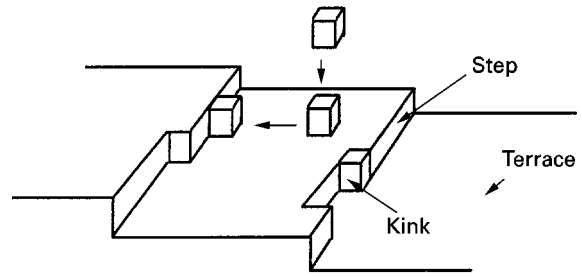


Figure 6 Diffusion of a growth unit towards and integration into the crystal surface layer.

Note that $G = dL/dt = 2 \bar{R}_{lin}$ for substitution of the linear rate equations in the population balance equation.

Crystal growth mechanisms For growth from solution the crystal growth processes can be roughly divided into two steps (Figure 6):

1. (volume) diffusion of growth units towards the crystal–solution interface
2. subsequent integration of these growth units into the crystal surface

The concentration profile perpendicular to the crystal surface is given in Figure 7, where the concentrations in the bulk at the crystal–solution interface and the equilibrium concentration at the growth site are indicated by c_b , c_i and c^* respectively.

For very soluble compounds, the growth rate is only limited by diffusion through the stagnant layer with thickness δ at the interface, with $c_b - c^*$ as the driving force for diffusion. For poorly soluble compounds the surface integration step is growth-limiting, and the driving force for the integration equals $c_i - c^*$. For most compounds, however, both steps must be taken into account. For growth from the melt the transport of the heat of crystallization becomes a third rate-limiting step. This is also the case for very concentrated solutions. In the following, first the surface integration and volume diffusion growth mechanisms and the related growth rate

expressions will be given, as well as the growth rate expressions for a combination of both steps. The expressions for heat transfer-controlled growth and for simultaneous heat and mass transfer will not be discussed here.

Surface integration controlled growth

Rough surfaces The structure of a growing surface at a molecular level is influenced by several factors: first, by the binding energies between the atoms, ions or molecules in the crystal surface layer. Also the solvent, temperature and driving force can play an important role. Depending on these factors, surfaces can become roughened. For a given compound and a selected solvent, either thermal or kinetic roughening may occur.

Each crystal face has a critical temperature above which the surface becomes rough. For ionic compounds these temperatures are very high, and always above the normal operating conditions. For organic compounds, however, roughening temperatures can even be close to room temperature, as with paraffin crystals growing from hexane. For rough growth the crystal faces tend to become rounded, especially at the edges, and nicely faceted crystals are no longer formed.

Kinetic roughening is caused by growth at too high supersaturation, and also happens for ionic substances. Rough growth always affects the crystal quality in a negative way, in particular the crystal purity, since impurities or solvent molecules are more easily incorporated.

It is not surprising that for rough growth the linear growth rate depends linearly on the supersaturation, because all surface sites can act as growth sites, and the rate constant k_r is proportional to the solubility of the compound. The solubility reflects the number of growth units that potentially impinges on the crystal surface, and thus contributes to its growth. The linear growth rate is given by:

$$R_{\text{lin}} = k_r \sigma \quad [59]$$

Smooth surfaces For growth of smooth crystal faces, as normally happens under moderate operating conditions, an orderly deposition of subsequent growth layers is needed. This can be realized by the propagation of growth steps along the crystal surface (Figure 6). Two sources can be identified for the generation of steps, and the two mechanisms of layered crystal growth are named after these sources: the 'birth and spread' or two-dimensional (2D) nucleation and growth model or the spiral growth model.

In the birth and spread model the steps are generated by the formation of 2D nuclei on the crystal surface that grow into islands by spreading laterally along the crystal surface. New nuclei can be formed on the original surface as well as on top of the already growing island. 2D nuclei can only be formed if the supersaturation is high enough to overcome the 2D nucleation barrier. The linear growth rate is given by:

$$R_{\text{lin}} = k_r (S - 1)^{2/3} S^{1/3} \exp\left(-\frac{B_{2D}}{3 \ln S}\right) \quad [60]$$

where $S = \sigma + 1$.

At low supersaturations, where 2D nuclei are not yet formed, screw dislocations that are present as lattice defects in the crystals and emerge on the crystal surface will act as step sources. The steps will curve around the defect emerging point, and spiral hillocks are formed.

The linear growth rate, also known as the parabolic growth law, equals:

$$R_{\text{lin}} = k_r \sigma^2 \quad [61]$$

In both eqns [60] and [61] k_r is directly proportional to the solubility of the compound. This solubility dependence is clearly seen in plots of the growth rates and the mean crystal sizes of many salts versus the supersaturation, as given by Mersmann. So, at the low supersaturations generally prevailing in evaporative and cooling crystallization, the surface integration growth step mostly obeys the parabolic law. At higher supersaturations, 2D nucleation and growth take over. If, at very high supersaturations, the size of the 2D nuclei approaches that of one growth unit, rough growth occurs (Figure 8).

Volume diffusion controlled growth Because diffusion through the stagnant boundary layer at the crystal surface is the rate-limiting step, this

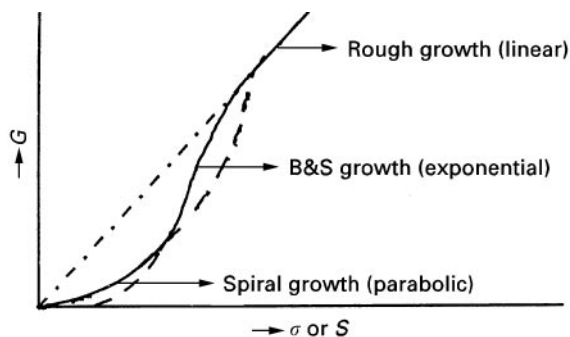


Figure 8 Growth curves for spiral, birth and spread (B&S) and rough growth.

growth model is also called the diffusion layer model. Even for rather concentrated solutions the simplified Fick's law can be applied, and the increase in crystal mass is given by:

$$\frac{dm}{dt} = \frac{D}{\delta} A(c_b - c^*) = k_d A(c_b - c^*) \quad [62]$$

The mass transfer coefficient k_d follows in its simplest form from $Sh = k_d L/D$, where for Sh several correlations provided in literature can be used. The values for Sh generally lie between 2 and 10. For concentrated solutions the Maxwell–Stefan equation is used

$$\frac{dm}{dt} = \frac{k_d}{(1-w)} A(c_b - c^*) \quad [63]$$

with w = mass fraction of the solute.

So, for most cases the linear growth rate is given by:

$$\bar{R}_{lin} = \frac{k_a k_d}{6k_v \rho} c^* \sigma \quad [64]$$

The dependency of \bar{R}_{lin} on σ is first order, and \bar{R}_{lin} is directly related to the solubility. It always limits the maximal growth rate by which a crystal can grow at a given supersaturation in Figure 8.

Volume diffusion and surface integration controlled growth For combined volume diffusion and rough growth as growth rate-determining steps, the growth process can be described by:

$$\frac{1}{A} \frac{dm}{dt} = \frac{k_d k_r}{k_d + k_r} (c_b - c^*) \quad [65]$$

while for combined volume diffusion and spiral growth surface integration the growth rate becomes:

$$\frac{1}{A} \frac{dm}{dt} = k_d (c_b - c^*) + \frac{k_d^2}{2k_r} - \left[\frac{k_d^4}{4k_r^2} + \frac{k_d^3 (c_b - c^*)}{k_r} \right]^{1/2} \quad [66]$$

With eqn [57] either \bar{R}_{lin} or G can be calculated.

The temperature dependence of k_r and k_d is given by an Arrhenius-type equation, where the corresponding Arrhenius activation energies are typically of the order of 40–60 kJ mol⁻¹ for surface integration and 10–20 kJ mol⁻¹ for the volume diffusion step.

For easily soluble compounds generally linear growth rates of 10⁻⁷ m s⁻¹ are permissible in order to

obtain smoothly grown crystals at σ values of 0.001 to 0.01, while for slightly soluble substances growth rates of 10⁻⁹ to 10⁻⁸ m s⁻¹ are commonly encountered at σ values of 10–100. Their corresponding mean sizes vary from 600 μ m to 10 μ m respectively.

Growth rate dispersion Small crystals, regardless whether they are born by primary or secondary nucleation, grow slower than their parent crystals. This is attributed to a certain content of stress in the small crystals. During the growth of the nuclei, the outer layers of the crystals lose some of the stress – a process called healing. Although the stress content of individual small crystals of the same size can differ, and thus their growth rate – a phenomenon named growth rate dispersion – the overall effect of stress on the growth rate of a large number of small crystals can equally be described by a size-dependent growth function. The equilibrium concentration then becomes a size-dependent function analogous to eqn [56].

$$G(L) = kg \left(\sigma - \frac{W_i(L)}{kT} \right)^g \quad [67]$$

where $W_i(L) = \Gamma_k/L_{fragment}$ and $g = 1$ for volume diffusion-dominated growth, and 2 for spiral growth. The value of Γ_k is, as mentioned before, a fitting parameter that has to be determined experimentally.

Dissolution of Crystals

Only at very low undersaturations or for extremely insoluble substances such as BaSO₄, the dissolution process proceeds by the disappearance of subsequent layers, and a smooth surface is maintained. Normally surface disintegration occurs at the crystal edges and at etch pits, and the surface becomes easily roughened. So the dissolution rate is either given by an expression where only volume diffusion is rate controlling:

$$-\frac{1}{A} \frac{dm}{dt} = k_d (c^* - c_b) \quad [68]$$

or by a combined volume diffusion and surface disintegration rate, as given by eqn [65] and, more rarely, by eqn [66], but now with a negative value for the change in mass, and a decreasing A .

Agglomeration

The agglomeration process consists of the transportation and collision of particles, and the attachment of the particles, followed by either disruption or cemen-

Table 2 Predominant agglomeration models for the possible transport mechanism as a function of particle size L and the Kolmogorov length scale η

Transport mechanism	Particle size L	Collision mechanism
Brownian motion	$L < 0.5 \mu\text{m}$	Perikinetic
Laminar flow	$L < 6 \eta$	Orthokinetic
Laminar flow	$L > 25 \eta$	Inertial
Turbulent flow	$L < 6 \eta$	Orthokinetic
Turbulent flow	$L > 25 \eta$	Inertial
Relative particle settling	$L < 6 \eta$	Inertial

tation of the attached particles. The cemented particles are agglomerates. If the supersaturation is zero, no cementation occurs and all loosely agglomerated particles fall apart again. Since in practice only the combined result of disruption and cementing can be observed, an effective agglomeration rate is generally defined.

The main transport mechanisms by which particles can collide are Brownian motion, laminar or turbulent flow or relative particle setting. Depending on the particle size and the Kolmogorov length scale of the different flow regimes, different collision mechanisms can be distinguished (Table 2).

In case of orthokinetic collisions the effective agglomeration rate constant or agglomeration kernel can be described as a product of the collision rate constant and an efficiency factor:

$$\beta = \psi(\varepsilon, \sigma)\beta_{\text{coll}} \quad [69]$$

β_{coll} increases linearly with the shear rate γ , that equals $\sqrt{\varepsilon/\nu}$ in a stirred vessel, whereas the efficiency factor ψ decreases strongly with γ in this high shear region, and thus β also decreases after having reached a maximal value at a rather low shear rate value. Although β should be size-dependent, experimental agglomeration data can often be fitted with a size-independent kernel. Hounslow and co-workers recently introduced a dependence of β_{coll} on the mean particle size. The efficiency factor includes the supersaturation dependence that is needed for the cementation of the particles. The supersaturation-dependent cementation explains why, for large crystallizers with a sufficiently large circulation time between two subsequent collisions with the impeller blades, abundant agglomeration may occur, while hardly any agglomeration is noticed for small scale crystallizers.

It must also be kept in mind that agglomeration is a kinetic process that depends on collisions, and thus on the local turbulence or power input ε . Averaging the power input ε for the calculation of β might

therefore lead to a wrong estimation of the degree of agglomeration.

Industrial Crystallizers

Several types of crystallizers are commercially available. The choice of crystallizer depends on the material to be crystallized and the solvent, the method of crystallization, the product specifications, in particular the crystal size distribution, and the flexibility of the design in cases where products of various coarseness (L_{50}) must be crystallized on demand in the same equipment.

Here only three large scale evaporative and cooling crystallizers will be discussed. These examples mainly serve to illustrate that in practice and in particular for a large scale crystallizer several compartments can be distinguished, where different processes may dominate.

Forced Circulation Crystallizer

The forced circulation (FC) crystallizer is the most widely used crystallizer. It is most common in multi-stage flash evaporative crystallization of salts with a flat solubility curve. It is the least expensive vacuum crystallizer, especially for evaporation of substantial amounts of water. The crystallizer as depicted in Figure 9 comprises two separate bodies that can be designed separately for evaporation and crystallization and for heat input.

The boiling zone with often a tangential inlet of the incoming flow should be large enough for vapour

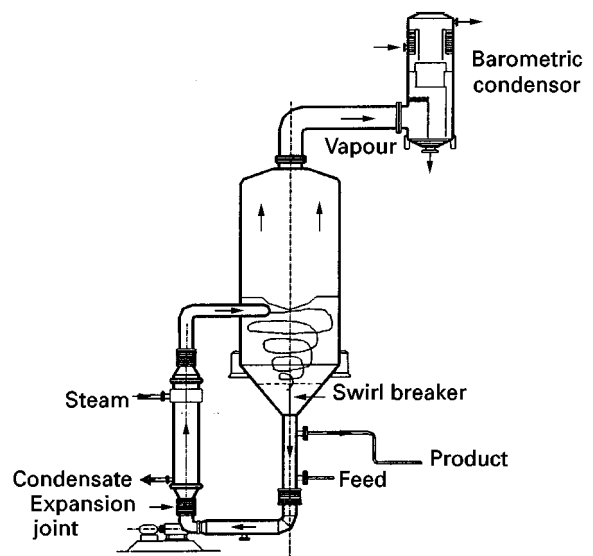


Figure 9 Forced circulation crystallizer with a tangential inlet (Swenson type). Reproduced with permission from Bennett (1993).

release, while the vessel bulk zone should maintain a sufficiently large volume to retain the growing crystals until the supersaturation is consumed. A slurry pump circulates the crystal slurry through the tubes of the heat exchanger, that can act as an internal fines dissolver, back into the boiling zone. This pump also creates most of the attrition fragments that may grow out as secondary nuclei, although usually an (axial-type) centrifugal pump is applied to minimize the attrition in order to get a sufficiently large mean crystal size. Because the forced circulation causes good mixing, the FC crystallizer is often modelled as a one compartment or MSMPR crystallizer in spite of its various zones.

The supersaturation and the turbulence may however differ locally.

Draft Tube Baffled Crystallizer

In this draft tube baffled (DTB) crystallizer with an external heat exchanger, as depicted in Figure 10, the heat duty is also separated from the crystallizer body. Fines removal has been realized by installing a skirt baffle that creates a settling or annular zone. The flow in the draft tube thus has to be upwards: this is effected by the impeller that also creates most of the attrition fragments. The fines flow can be diluted or heated to partly or totally dissolve

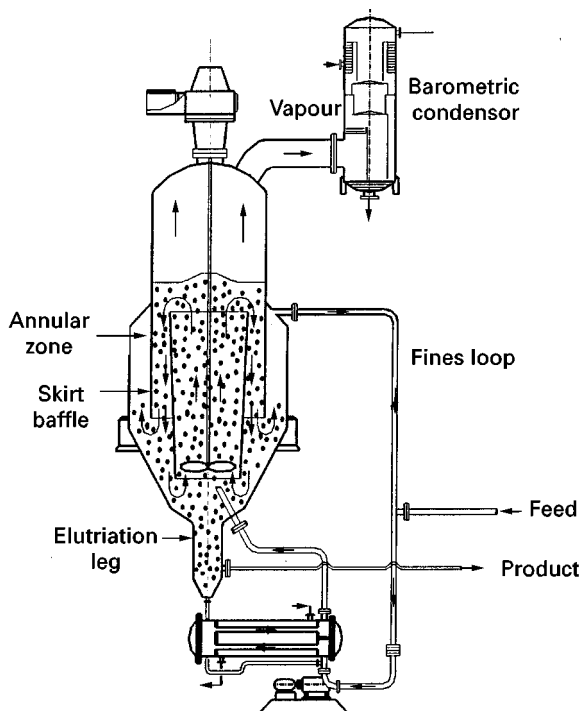


Figure 10 Stirred draft tube baffle (DTB) crystallizer with an external heat exchanger and fines destruction (Swenson type). Reproduced with permission from Bennett (1993).

the fines. An increase in fines flow increases the number of fines that are removed from the crystallizer, but also the cut size of the fines. The fines loop in this way serves as an actuator that can be applied for control of the mean crystal size, although the variation in mean crystal size that can be achieved is limited.

The addition of an elutriation leg at the bottom of the crystallizer or the addition of another type of classifier allows classification of the product flow, and thus also serves as an actuator to influence the CSD of the product.

Obviously the various zones of the DTB crystallizer have different functions, and different supersaturation and turbulence values can be expected, in particular for large scale crystallizers.

The DTB crystallizer can also be applied as cooling crystallizer by using the heat exchangers as a cooling system.

Fluidized Bed Crystallizer

A fluidized bed crystallizer (Figure 11) is especially designed to produce large and uniformly sized crystals. The heat duty and the crystallizer body are again separated. At the top of the bed the crystals are settled, and only the fines leave the crystallizer with the exhausted mother liquor to be circulated through the heat exchanger after mixing with the feed stream. The hot circulated flow enters the vaporizer head, where the solvent is flashed off. The supersaturated solution leaves the vaporizer through the downcomer, and enters the densely packed fluidized bed at the bottom of the crystallizer. The supersaturation is consumed on its way up, and a coarse product leaves the crystallizer at the bottom.

Secondary nucleation here results from crystal-crystal collisions. Also for this crystallizer several functions can be identified that are restricted to various zones in the crystallizer. The supersaturation and the turbulence are also not evenly distributed.

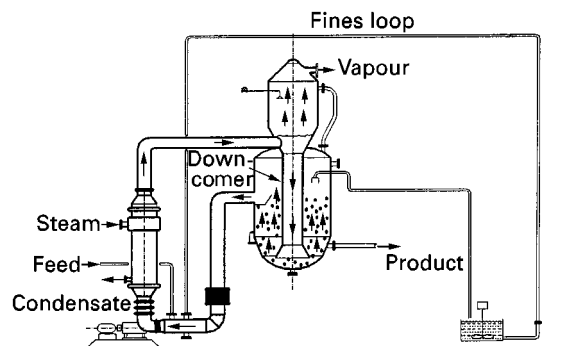


Figure 11 Fluidized bed crystallizer (Swenson type). Reproduced with permission from Bennett (1993).

Since the residence time of the crystals can be considerably increased, this type of crystallizer is commonly used to produce large crystals.

This crystallizer can also be used for cooling crystallization. No vapour chamber is then needed. Other well-known cooling crystallizers are: first, a Swenson type where the suspension is circulated through a heat exchanger; second, a direct cooling crystallizer, where a refrigerant is introduced directly into a draft tube crystallizer; and third, a cooling disc crystallizer, that can be regarded as a compact cascade of cooling crystallizers with various cooling elements that are scraped by rotating wipers.

Compartmental Modelling

In an industrial crystallizer various zones with different functions can be identified, as has been illustrated in the former section. The supersaturation (Kramer *et al.* 1999) and the turbulence (Derksen and van den Akker, 1999) in a crystallizer are therefore not necessarily evenly distributed. Their local values depend on the geometry and scale of the crystallizer,

on the flow pattern, as well as on the rates of the kinetic processes and the production rate of the specific crystallizing compound. In particular, the nonlinear kinetic processes such as nucleation and agglomeration are strongly dependent on these local values. It also has to be established whether locally the supersaturation does not exceed a maximum beyond which value rough growth occurs or too many solvent inclusions are incorporated in the crystals.

As the conventional modelling techniques use geometrically lumped descriptions (i.e. MSMR) of the physical processes inside a crystallizer vessel (Randolph, 1998; Mersmann, 1995; Eek, 1995; O'Meadhra, 1996), they do not account for the variations in the local process conditions and have therefore seldom proven to be reliable for scale-up purposes. A reliable tool for modelling of crystallizers requires the separation of kinetics and hydrodynamics. A well-known technique for this purpose is compartmental modelling. This technique, which is frequently applied for standard reactor engineering problems, has been applied within crystallization for a number of years (Kramer, 1999).

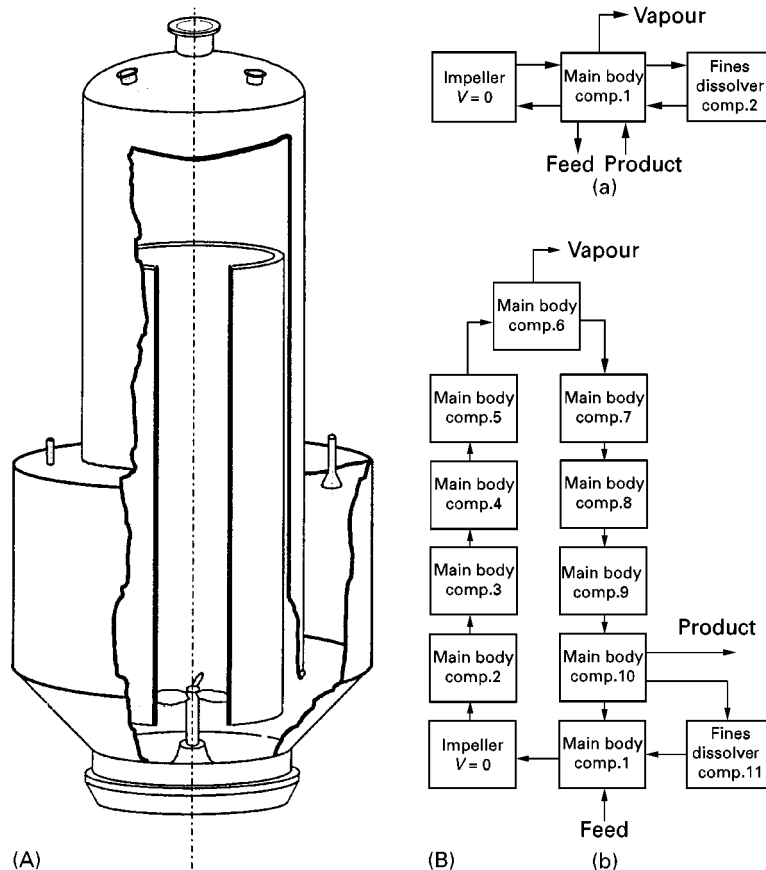


Figure 12 (A) A DTB crystallizer and (B: a,b) two compartment structures.

Here an example will be presented to illustrate the design of a compartment model for a 360 m³ DTB crystallizer, with the main crystallizer body modelled as a one- or as a multicompartment vessel.

The subdivision of the crystallizer into multiple compartments is performed on the basis of crystallizer geometry, hydrodynamic analysis and characteristic times of the crystallization kinetics (Kramer 1999). In compartmental modelling, process conditions may differ between compartments but not within compartments, because the individual compartments are modelled as well-mixed vessels. A three-step approach is used to define the size and location of the compartments as well as the exchange flow rates between them:

1. Set up a rough compartment structure on the basis of the crystallizer geometry, e.g. an inlet compartment, a propeller compartment, a boiling zone compartment, etc.
2. Compare the characteristic time of supersaturation depletion due to crystal growth with the residence time in each compartment to check the constant supersaturation assumption. If necessary, the compartment structure may be refined.
3. Use computational fluid dynamic (CFD) results to refine further the compartment structure, specifically with respect to the exchange flow rates and the constant energy dissipation assumption in each compartment.

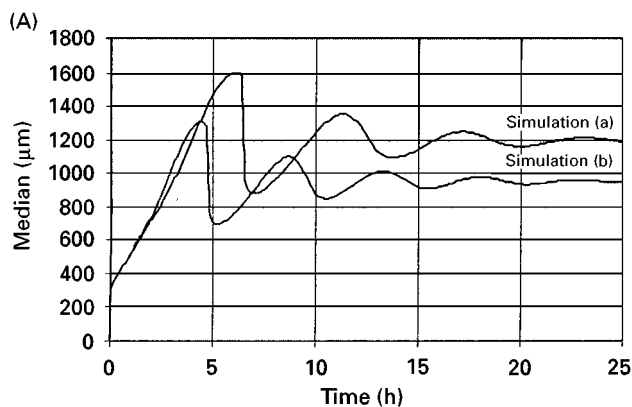
The importance of compartmental modelling is illustrated for a 360 m³ DTB crystallizer (Figure 12)

with ammonium sulfate and water as the model system. This crystallization system is dominated by secondary nucleation and growth. The model framework of Gahn and Mersmann (see section on secondary nucleation, above) is the most sophisticated for such systems and is hence used in this example. Figure 12 also contains two compartment structures for this DTB crystallizer. The first compartment structure (Figure 12B a) describes a MSMPR crystallizer with fines removal and fines dissolution. The second structure (Figure 12B b) was created using the three-step approach presented in the previous paragraph.

Both compartment structures will now be used to describe the behaviour of the 360 m³ DTB crystallizer operating with a residence time of 75 min, an impeller frequency of 45 rpm and a fines withdrawal rate of 157 m³ min⁻¹. Additional information regarding the equipment, operating conditions and simulation details can be found in Bermingham *et al.* (1999).

Results of simulations with both compartment structures are depicted in Figure 13. Taking the spatial distribution of the supersaturation into account clearly has a large influence on the predicted crystal size distribution. The lower median size of simulation (b) is most probably related to the higher supersaturation of the withdrawn fines flow, i.e. 1.78 as opposed to 1.38 kg m⁻³. Furthermore, it is interesting to note that a large majority of the crystal mass is produced in only half the crystallizer volume.

This example clearly illustrates the effect of varying process conditions in different zones of an industrial crystallizer on the CSD of the produced



(B)

	Crystal mass production (kg m ⁻³ s ⁻¹)	Supersaturation, $c-c^*$ (kg m ⁻³)
Simulation (a)		
MB-C1	0.0434	1.38
FD-C2	-0.0478	-4.03
Simulation (b)		
MB-C1	0.0008	0.23
MB-C2	0.0007	0.24
MB-C3	0.0007	0.23
MB-C4	0.0007	0.23
MB-C5	0.0007	0.23
MB-C6	0.1118	2.66
MB-C7	0.0964	2.41
MB-C8	0.0834	2.18
MB-C9	0.0725	2.00
MB-C10	0.0799	1.78
FD-C11	-0.0512	-3.60

Figure 13 (A) Dynamic trend of the median crystal size and (B) steady-state crystal mass production and supersaturation for simulations (a) and (b).

crystals. Compartmental modelling is therefore an important or even essential tool in the design of industrial crystallizers to predict the influence of crystallizer geometry, scale, operating conditions and process actuators on the process behaviour and product quality.

Only using this approach can a reasonable prediction can be obtained for the composition of the bleed and/or product streams, and of the filterability and washability of the product, which determine the efficiency of this separation process.

Product Properties Related to the Process Conditions

In order to apply crystallization as an adequate separation process, the solid phase has to fulfil a number of requirements. The crystal size distribution as well as the shape of the crystals should meet the demands of a good filterability and washability of the product, as is needed for a good separation. The surface roughness of the crystals may also play a role, because a rough surface leads to attrition, and the attrited fragments may hamper the downstream processes.

The crystals should be formed under process conditions that minimize the uptake of impurities or mother liquor inclusions in the crystals. This can happen when the (local) supersaturation is too high. A too high local turbulence should be avoided, this causes attrition of especially the corners or edges of the crystals. Although healing of the crystals will occur particularly in the regions of the highest supersaturations, this healing process is never perfect, and always leads to the uptake of solvent inclusions. That crystals are prone to attrition beyond a certain size that also depends on the degree of turbulence can be seen from Figure 14.

Agglomeration should in general be prevented, since liquid incorporation between the primary par-

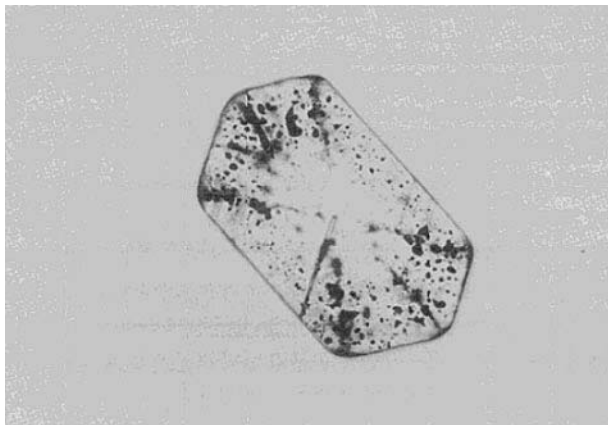


Figure 14 Liquid inclusions in $(\text{NH}_4)_2\text{SO}_4$ crystal embedded in a liquid of similar refractive index.

ticles of an agglomerate is unavoidable. Only if, as often happens in precipitation processes, the primary particles are too small for filtration, agglomeration should just be promoted. In that event the solute concentration in the mother liquor is extremely low and some incorporation of it in the solid phase hardly affects the separation process.

Final Remarks

To summarize, it can be said that the design of a good evaporative or cooling crystallization process is based on heat, mass and population balances, kinetic processes of nucleation, growth and agglomeration of the particles, as well as on the hydrodynamics that exist in the crystallizer of a given geometry and scale. However, as the prevailing process conditions are not evenly distributed in industrial crystallizers, local descriptions of the crystallization phenomena are needed to calculate the local variations in the process conditions, their effect on the process performance and to predict their dependence of the scale and geometry of the crystallizer. It has been shown that by taking all these balances and processes into account in a compartmental modelling tool, the efficiency of the separation process as well as the quality of the crystalline product and the process performance can be properly predicted.

Symbols

a	activity	J mol^{-1}
A	primary nucleation factor	$\# \text{m}^{-3} \text{s}^{-1}$
A_T	total crystal surface area per unit crystallizer volume	$\text{m}^2 \text{m}^{-3}$
$B(\varepsilon, \nu)$	breakage function	$\# \text{m}^{-1}$
B_0	birth rate	$\# \text{m}^{-3} \text{s}^{-1}$
$B(L)$	birth rate (size-based)	$\# \text{m}^{-3} \text{m}^{-1} \text{s}^{-1}$
$B(\nu)$	birth rate (volume-based)	$\# \text{m}^{-3} \text{m}^{-3} \text{s}^{-1}$
c	concentration	kg m^{-3}
C_p	specific heat	$\text{J kg}^{-1} \text{K}^{-1}$
$D(L, t)$	death rate	$\# \text{m}^{-3} \text{m}^{-1} \text{s}^{-1}$
$D(\nu, t)$	death rate	$\# \text{m}^{-3} \text{m}^{-3} \text{s}^{-1}$
G_L or G	linear growth rate	m s^{-1}
G_V	volumetric growth rate	$\text{m}^3 \text{s}^{-1}$
H	enthalpy	—
$H(L)$	classification function	—
J	primary nucleation rate	$\# \text{m}^{-3}$
k	Boltzmann constant	J K^{-1}
k_a, k_v	surface, volume shape factor	—
k_n or k_v^*	nucleation rate constant	—
k_{distr}	distribution constant impurity uptake	—

L	particle length	m
L_D	dominant crystal size	m
L_T	total crystal length per unit crystallizer volume	m m^{-3}
m_j	j th moment of a distribution	...
M_T	total crystal mass per unit crystallizer volume	kg m^{-3}
$m(L)$	mass density	$\text{kg m}^{-3} \text{m}^{-1}$
$m(v)$	mass density	$\text{kg m}^{-3} \text{m}^{-3}$
$n(L)$	number density	$\# \text{m}^{-3} \text{m}^{-1}$
$n(v)$	number density	$\# \text{m}^{-3} \text{m}^{-3}$
N_T	total number of crystals	$\# \text{m}^{-3}$
P	production rate	kg s^{-1}
r	radius	m
$r(v_1, v_2)$	rate of aggregation	$\# \text{m}^{-9} \text{s}^{-1}$
R	gas constant	$\text{J mol}^{-1} \text{K}^{-1}$
R_{lin}	linear growth rate of a crystal face	m s^{-1}
S	supersaturation ratio	—
$S(v)$	selection function	s^{-1}
t	time	s
T	temperature	K
u	particle volume	m^3
v	particle volume	m^3
V	crystallizer volume	m^3
V_T	total crystal volume per unit crystallizer volume	$\text{m}^3 \text{m}^{-3}$
V_{molar}	molar volume	$\text{m}^3 \text{mol}^{-1}$
w	mass fraction	—
W_i	stress energy crystals	J
β	aggregation kernel	$\text{m}^3 \text{s}^{-1}$
γ	interfacial free energy, activity coefficient	J m^{-2} , —
ε	specific power input impeller	W m^{-3}
η	Kolmogorof length scale	m
ϕ_v	volumetric flow rates	$\text{m}^3 \text{s}^{-1}$
μ	chemical potential	J mol^{-1}
ρ	material density	kg m^{-3}
σ	relative supersaturation	—
τ	residence time	s
ψ	efficiency factor for agglomeration	—
Γ_k	surface-related stress	Jm

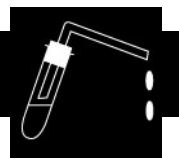
See Colour Plate 4.

Further Reading

- Arkenbout GF (1995) *Melt Crystallization Technology*. Lancaster, USA: Technomic.
- Becker R and Göring W (1935) Kinetische Behandlung der Keimbildung in übersättigten Dämpfen. *Ann Physik* 24: 719–752.
- Bennema P (1993) Growth and morphology of crystals. In: Hurle DTJ (ed.) *Handbook of Crystal Growth*, vol. 1A, pp. 477–583. Amsterdam: Elsevier Science.
- Bennett RC (1993) Crystalliser selection and design. In: Meyerson A (ed.) *Handbook of Industrial Crystallisation*, pp. 103–130. Boston: Butterworth Heinemann.
- Birmingham SK, Neumann AM, Kramer HJM *et al.* (1999) A design procedure and predictive models for solution crystallisation processes. In: *Proceedings of Fifth International Conference on Foundations of Computer Aided Process Design, FOCAPD'99*, Breckenridge, USA, paper I21.
- Derksen J and van den Akker HEA (1999) Large eddy simulations on the flow driven by a rushton turbine. *AIChE Journal* 45: 209–221.
- Eek RA, Dijkstra SJ and van Rosmalen GM (1995) Dynamic modelling of suspension crystallisers, using experimental data. *AIChE Journal* 41: 571–584.
- Gahn C and Mersmann A (1997) Theoretical prediction and experimental determination of attrition rates. *Transactions IChemE* 75(A): 125–131.
- Gahn C and Mersmann A (1999) Brittle fracture in crystallisation processes. Part A. Attrition and abration of brittle solids. *AIChE Journal* 54: 1273–1282.
- Gahn C and Mersmann A (1999b) Brittle fracture in crystallisation processes. Part B. Growth of fragments and scale up of suspensions crystallisers. *AIChE Journal* 54: 1283–1292.
- Hounslow MJ (1998) The population balance as a tool for understanding particle rate processes. *KONA* 16: 179–193.
- Hounslow MJ, Mumtaz HS, Collier AP, Barrick JP and Bramley AS (1999) Aggregation during precipitation – putting the pieces of the puzzle together. Proceedings of the 14th International Symposium on Industrial Crystallization, CD ROM.
- Hurle D (1993) *Handbook of Crystal Growth*. Amsterdam: Elsevier Science.
- Ilievski D and Hounslow MJ (1995) Tracer studies of agglomeration during precipitation. Part II: Quantitative analysis of tracer data and identification of mechanism. *AIChE Journal* 41: 525–535.
- Kashchiev D (2000) *Nucleation: Theory and Application*. Oxford: Butterworth Heinemann.
- Kind M and Mersmann A (1990) On supersaturation during mass crystallisation form solution. *Chemical Engineering Technology* 13: 50–62.
- Kramer HJM, Dijkstra JW, Neumann AM *et al.* (1996) Modelling of industrial crystallizers, a compartmental approach using a dynamic flow-sheet tool. *Journal of Crystal Growth* 166: 1084–1088.
- Kramer HJM, Birmingham SK and van Rosmalen GM (1999) Design of industrial crystallisers for a required product quality. *Journal of Crystal Growth* 198/199: 729–737.
- Litster, JD, Smit DJ and Hounslow MJ (1995) Adjustable discretized population balance for growth and aggregation. *AIChE Journal* 41: 591–603.

- Mersmann A (1988) Design of crystallisers. *Chemical Engineering Process* 23: 213–228.
- Mersmann A (1995) *Crystallisation Technology Handbook*. New York: Marcel Dekker.
- Meyerson AS (1993) *Handbook of Industrial Crystallisation*. Boston: Butterworth Heinemann.
- Mullin JW (1993) *Crystallisation*. Boston: Butterworth Heinemann.
- Mumtaz HS, Hounslow, MJ, Seaton NA and Paterson WR (1997) Orthokinetic aggregation during precipitation: a computational model for calcium oxalate. *Transactions of the IChemE* 75: 152–159.
- Mutaftschiev B (1993) Nucleation theory. In: Hurle DTJ (ed.) *Handbook of Crystal Growth*, vol. 1A, pp. 187–247. Amsterdam: Elsevier.
- Nicmanis M and Hounslow MJ (1998) Finite-element methods for steady-state population balance equations. *AIChE Journal* 44: 2258–2272.
- Nyvtl J (1992) *Design of Crystallisers*. Boca Raton, FL: CRC Press.
- Ó Meadhra R, Kramer HJM and van Rosmalen GM (1996) A model for secondary nucleation in a suspension crystalliser. *AIChE Journal* 42: 973–982.
- Ottens EPK, Janse AH and De Jong EJ (1972) Secondary nucleation in a stirred vessel cooling crystalliser. *Journal of Crystal Growth* 13/14: 500–505.
- Ploß R, Tengler T and Mersmann A (1989) A new model of the effect of stirring intensity on the rate of secondary nucleation. *Chemical Engineering Technology* 12: 137–146.
- Randolph AD and Larson MA (1988) *Theory of Particulate Processes*. 2nd edn. New York: Academic Press.
- Sinnott RK (1998) In: *Chemical Engineering Design*, vol. 6. (Coulson JM and Richardson JF eds.), Oxford: Butterworth Heinemann.
- Söhnle O and Garside J (1992) *Precipitation*. Oxford: Butterworth Heinemann.
- van der Eerden JP (1993) Crystal growth mechanisms: In: Hurle DTJ (ed.) *Handbook of Crystal Growth*, vol. 1A, pp. 307–477. Amsterdam: Elsevier Science.
- van der Heijden AEDM, van der Eerden JP and van Rosmalen GM (1994) The secondary nucleation rate; a physical model. *Chemical Engineering Science* 3103–3113.
- Volmer M (1939) *Kinetik der Phasenbildung*. Dresden: Steinkopf.

DISTILLATION



R. Smith and M. Jobson, Department of Process Integration, UMIST, Manchester, UK

Copyright © 2000 Academic Press

Introduction

Distillation is the most commonly used method for the separation of homogeneous fluid mixtures. Separation exploits differences in boiling point, or volatility, between the components in the mixture. Repeated vaporization and condensation of the mixture allows virtually complete separation of most homogeneous fluid mixtures. The vaporization requires the input of energy. This is the principal disadvantage of distillation: its high energy usage. However, distillation has three principle advantages over alternative methods for the separation of homogeneous fluid mixtures:

1. The ability to handle a wide range of feed flow rates. Many of the alternative processes for the separation of fluid mixtures can only handle low flow rates, whereas distillation can be designed for the separation of extremely high or extremely low flow rates.

2. The ability to separate feeds with a wide range of feed concentrations. Many of the alternatives to distillation can only separate feeds that are already relatively pure.
3. The ability to produce high product purity. Many of the alternatives to distillation only carry out a partial separation and cannot produce pure products.

It is no accident that distillation is the most common method for the separation of homogeneous mixtures. It is a versatile, robust and well-understood technique. We shall start explaining distillation by a single-stage separation, before understanding how to set up a cascade of separation stages, which is distillation.

Single-Stage Separation

Consider the liquid mixture illustrated in **Figure 1**. If this liquid mixture is partially vaporized then the vapour becomes richer in the more volatile components (i.e. those with the lower boiling points) than the liquid phase. The liquid becomes richer in the less volatile components (i.e. those with the higher boiling points). If we allow the system in **Figure 1** to come to equilibrium conditions, then the distribution of the components between the vapour and liquid phases is